

# Ionospheric effects of the solar flares as deduced from global GPS network data

L.A. Leonovich, A.T. Altynsev, V.V. Grechnev, E. L. Afraimovich  
 Institute of Solar-Terrestrial Physics SD RAS,  
 p. o. box 4026, Irkutsk, 664033, Russia  
 fax: +7 3952 462557; e-mail: lal@iszf.irk.ru

## Abstract

Results derived from analysing the ionosphere response to faint and bright solar flares are presented. The analysis used technology of a global detection of ionospheric effects from solar flares as developed by the authors, on the basis of phase measurements of the total electron content (TEC) in the ionosphere using an international GPS network. The essence of the method is that use is made of appropriate filtering and a coherent processing of variations in the TEC which is determined from GPS data, simultaneously for the entire set of visible GPS satellites at all stations used in the analysis. This technique is useful for identifying the ionospheric response to faint solar flares (of X-ray class C) when the variation amplitude of the TEC response to separate line-on-sight to GPS satellite is comparable to the level of background fluctuations. The dependence of the TEC variation response amplitude on the flares location on the Sun is investigated.

## 1 Introduction

The enhancement of X-ray and ultraviolet (UV) emission that is observed during chromospheric flares on the Sun immediately causes an increase in electron density in the ionosphere. These density variations are different for different altitudes and are called Sudden Ionospheric Disturbances, SID, (Davies, 1990), (Donnelly, 1969). SIDs are generally recorded as the short wave fadeout, SWF, (Stonehocker, 1970), sudden phase anomaly, SPA, (Ohshio, 1971), sudden frequency deviation, SFD, (Donnelly, 1971), (Liu et al., 1996), sudden cosmic noise absorption, SCNA, (Deshpande and Mitra, 1972), sudden enhancement/decrease of atmospherics, SES, (Sao et al., 1970). Much research is devoted to SID studies, among them a number of thorough reviews (Mitra, 1974), (Davies, 1990).

SFD are caused by an almost time-coincident increase in  $E$ - and  $F$ -region electron densities at over 100 km altitudes covering an area with the size comparable to or exceeding that of the region monitored by the system of HF radio paths (Davies, 1990), (Donnelly, 1969), (Liu et al., 1996). A limitation of this method is the uncertainty in the spatial and altitude localization of the UV flux effect, the inadequate number of paths, and the need to use special-purpose equipment.

The effect of solar flares on the ionospheric  $F$ -region is also manifested as a Sudden Increase of Total Electron Content, SITEC, which was measured previously using continuously operating VHF radio beacons on geostationary satellites (Mendillo et al., 1974), (Davies, 1980). A serious limitation of methods based on analyzing VHF signals from geostationary satellites is their small and ever increasing (with the time) number and the nonuniform distribution in longitude. Hence it is impossible to make measurements in some geophysically interesting regions of the globe, especially in high latitudes.

A further, highly informative, technique is the method of Incoherent Scatter - IS (Mendillo et al., 1974), (Thome et al., 1971). However, the practical implementation of the IS method requires very sophisticated, expensive equipment. An added limitation is inadequate time resolution. Since the relaxation time of electron density in the  $E$  and  $F1$  regions is also less than 5-10 min, most IS measurements lack time resolution needed for the study of ionospheric effects of flares.

Consequently, none of the above-mentioned existing methods can serve as an effective basis for the radio detection system to provide a continuous, global SID monitoring with adequate space-time resolution. Furthermore, the creation of these facilities requires developing special purpose equipment, including powerful radio transmitters contaminating the radio environment. It is also significant that when using the existing methods, the inadequate spatial aperture gives no way of deducing the possible spatial inhomogeneity of the X-ray and UV flux.

The advent and evolution of a Global Positioning System (GPS) and also the creation on its basis of widely branched networks of GPS stations (at least 800 sites at the February of 2001, the data from which are placed on the Internet) opened up a new era in remote ionospheric sensing. High-precision measurements of the TEC along the line-of-sight (LOS) between the receiver on the ground and transmitters on the GPS system satellites covering the reception zone are made using two-frequency multichannel receivers of the GPS system at almost any point of the globe and at any time simultaneously at two coherently coupled frequencies  $f_1 = 1575.42$  MHz and  $f_2 = 1227.60$  MHz.

The sensitivity of phase measurements in the GPS system is sufficient for detecting irregularities with an amplitude of up to  $10^3 - 10^4$  of the diurnal TEC variation. This makes it possible to formulate the problem of detecting ionospheric disturbances from different sources of artificial and natural origins. The TEC unit (TECU) which is equal to  $10^{16} \text{m}^{-2}$  and is commonly accepted in the literature, will be used throughout the text.

Afraimovich et al. (2000a, 2000b, 2001) developed a novel technology of a global detection of ionospheric effects from solar flares and presented data from first GPS measurements of global response of the ionosphere to powerful impulsive flares of July 29, 1999, and December 28, 1999, were chosen to illustrate the practical implementation of the proposed method. Authors found that fluctuations of TEC, obtained by removing the linear trend of TEC with a time window of about 5 min, are coherent for all stations and LOS on the dayside of the Earth. The time profile of TEC responses is similar to the time behavior of hard X-ray emission variations during flares in the energy range 25-35 keV if the relaxation time of electron density disturbances in the ionosphere of order 50-100 s is introduced. No such effect on the nightside of the Earth has been detected yet.

The objective of this paper is to use this technology for analysing the ionosphere response to faint and bright solar flares.

## 2 Processing of the data from the GPS network

Following is a brief outline of the global monitoring (detection) technique for solar flares. A physical groundwork for the method is formed by the effect of fast change in electron density in the Earth's ionosphere at the time of a flare simultaneously on the entire sunlit surface. Essentially, the method implies using appropriate filtering and a coherent processing of TEC variations in the ionosphere simultaneously for the entire set of visible (during a given time interval) GPS satellites (as many as 5-10 satellites) at all global GPS network stations used in the analysis.

In detecting solar flares, the ionospheric response is virtually simultaneous for all stations on the dayside of the globe within the time resolution range of the GPS receivers (from 30 s to 0.1 s). Therefore, a coherent processing of TEC variations implies in this case a simple addition of single TEC variations. The detection sensitivity is determined by the ability to detect typical signals of the ionospheric response to a solar flare (leading edge duration, period, form, length) at the level of TEC background fluctuations. Ionospheric irregularities are characterized by a power spectrum, so that background fluctuations will always be distinguished in the frequency range of interest. However, background fluctuations are not correlated in the case of beams to the satellite spaced by an amount exceeding the typical irregularity size. With a typical length of X-ray bursts and UV emission of solar flares of about 5-10 min, the corresponding ionization irregularity size does normally not exceed 30-50 km; hence the condition of a statistical independence of TEC fluctuations at spaced beams is almost always satisfied. Therefore, coherent summation of responses to a flare on a set of LOS spaced throughout the dayside of the globe permits the solar flare effect to be detected even when the response

amplitude on partial LOS is markedly smaller than the noise level (background fluctuations).

The proposed procedure of coherent accumulation is essentially equivalent to the operation of coincidence schemes which are extensively used in X-ray and gamma-ray telescopes. If the SID response and background fluctuations, respectively, are considered to be the signal and noise, then as a consequence of a statistical independence of background fluctuations the signal/noise ratio when detecting the flare effect is increased through a coherent processing by at least a factor of  $\sqrt{N}$ , where  $N$  is the number of LOS.

The GPS technology provides the means of estimating TEC variations on the basis of phase measurements of TEC  $I$  in each of the spaced two-frequency GPS receivers using the formula (Hofmann-Wellenhof et al., 1992), (Calais and Minster, 1996):

$$I = \frac{1}{40.308} \frac{f_1^2 f_2^2}{f_1^2 - f_2^2} [(L_1 \lambda_1 - L_2 \lambda_2) + const + nL] \quad (1)$$

where  $L_1 \lambda_1$  and  $L_2 \lambda_2$  are the increments of the radio signal phase path caused by the phase delay in the ionosphere (m);  $L_1$  and  $L_2$  stand for the number of complete phase rotations, and  $\lambda_1$  and  $\lambda_2$  are the wavelengths (m) for the frequencies  $f_1$  and  $f_2$ , respectively; *const* is some unknown initial phase path (m); and  $nL$  is the error in determining the phase path (m).

Phase measurements in the GPS system are made with a high degree of accuracy where the error in TEC determination for 30-second averaging intervals does not exceed  $10^{14} \text{m}^{-2}$ , although the initial value of TEC does remain unknown (Hofmann-Wellenhof et al., 1992).

This permits ionization irregularities and wave processes in the ionosphere to be detected over a wide range of amplitudes (as large as  $10^{-4}$  of the diurnal variation of TEC) and periods (from several days to 5 min). The TEC unit, *TECU*, which is equal to  $10^{16} \text{m}^{-2}$  and is commonly accepted in the literature, will be used throughout the text.

The data analysis was based on using the stations, for which the local time during the flare was within 10 to 17 LT. From 50 to 150 LOS were processed for each flare.

Primary data include series of slant values of TEC  $I(t)$ , as well as the corresponding series of elevations  $\theta(t)$  and azimuths  $\alpha(t)$  along LOS to the satellite calculated using our developed CONVTEC program which converts the GPS system standard RINEX-files on the INTERNET (Gurtner, 1993). The determination of SID characteristics involves selecting continuous series of  $I(t)$  measurements of at least a one-hour interval in length, which includes the time of the flare. Series of elevations  $\theta(t)$  and azimuths  $\alpha(t)$  of the LOS are used to determine the coordinates of subionospheric points. In the case under consideration, all results were obtained for elevations  $\theta(t)$  larger than  $30^\circ$ .

The method of coherent summation of time derivatives of the series of variations of the "vertical" TEC value was employed in studying the ionospheric response to solar flares. Our choice of the time derivative of TEC was motivated by the fact this derivative permits us to get rid of a constant component in TEC variations; furthermore, it reflects electron density variations that are proportional to the flux of ionizing radiation.

The coherent summation of time derivatives of the series of variations of the "vertical" TEC value was made by the formula:

$$Sw = \sum_{i=1}^n dI(t)/dt_i \times K_i \quad (2)$$

where  $n$  is the number of LOS. The correction coefficient  $K_i$  is required for converting the slant TEC to an equivalent "vertical" value (Klobuchar, 1986)

$$K_i = \cos \left[ \arcsin \left( \frac{R_z}{B_z + h_{\max}} \cos \theta_i \right) \right], \quad (3)$$

where  $R_z$  is Earth's radius; and  $h_{\max}$  is the height of the ionospheric  $F2$ -layer maximum.

Next the trend determined as a polynomial on a corresponding time interval is removed from the result (normalized to the number of LOS) of the coherent summation of the time derivatives. After that, the calculated time dependence ( $Sd_{ex}(t)$ ) is integrated in order to obtain the mean integral TEC increment  $\Delta I(t)$  on the time interval specified.

$$\Delta I(t) = \int_{t1}^{t2} Sd_{ex}(t) dt \quad (4)$$

This technique is useful for identifying the ionospheric response to faint solar flares (of X-ray class C) when the variation amplitude of the TEC response to separate LOS is comparable to the level of background fluctuations.

### 3 Ionospheric response to faint solar flares

An example of a processing of the data for a faint solar flare July 29, 1999 (C2.7/ SF, 11:11 GT, S16W11) is given in Figure 1. One hundred LOS were processed for the analysis of this event. Panels (a) and (b) present the typical time dependencies of TEC variations for separate LOS, and their time derivatives. The BRUS (PRN14, thick line) and BAHN (PRN29, thin line) stations are taken as our example. It is apparent from these dependencies that no response to the flare is distinguished in the TEC variations and in their time derivatives for the individual LOS, because the amplitude of the TEC response for the individual LOS is comparable to the level of background fluctuations.

A response to the solar flare is clearly seen in the time dependence (Figure 1c) which is a normalized result of a coherent summation  $Sd$  of the time derivatives of the TEC variations for all LOS. Upon subtracting the trend determined as a polynomial of degree 3 on the time interval 10:07-10:39 UT, the same curve (c) is presented in Figure 1d as  $Sd_{ex}(t)$ . Next the calculated time dependence was integrated over the time interval 10:07-10:39 UT to give the mean integral increment of TEC (Figure 1e, thick line). A comparison of the resulting dependence with the values of the soft X-ray emission flux (GOES-10) in the range 1-8 Å (Figure 1e, thin line) reveals that it has a more flattened form, both in its rise and fall. A maximum in X-rays is about 6 minutes ahead of that in TEC.

Examples of the application of our technology for the analysis of the ionospheric response to faint solar flares are given in Figures 2 and 3. Figure 2 gives the data processing results on TEC variations for solar flares : July 29, 1999 (C2.2, 11:00 UT) on panels a, b, c, d, and July 29, 1999 (C6.2/SN, 15:14 UT, N25E33 ) on panels e, f, g, h. Figure 3 shows the results of a data processing of TEC variations for solar flares of November 17, 1999 (C7.0/1N, 09:38 UT, S15W53) on panels a, b, c, d, and November 11, 1999 (C5.0, 15:40 UT) on panels e, f, g, h.

## 4 Ionospheric response to bright flares

An example of a processing of the data for the bright solar flare of July 14, 1998 (M4.6/1B, 12:59 UT, S23E20) is given in Figure 4.

Fifty LOS were used in the analysis of this event. Figure 4a presents the time dependencies of hard X-ray emission (CGRO/Batse, 25-50 keV, thick line on panels a ) and of the UV line (SOHO/SUMMER 171 Å, thin line) in arbitrary units (Aschwanden et al., 1999). It should be noted that the time dependence of the UV 171 Å line is more flattened, both in the rise and in the fall, when compared with the hard X-ray emission characteristic. The increase in the UV 171 Å line starts by about 1.8 minute earlier, and the duration of its disturbance exceeds considerably that of the hard X-ray emission disturbance.

Panel (b) presents the typical time dependencies of the TEC variations for separate LOS. The AOML (PRN24, thick line) and ACSI (PRN18, thin line) stations are taken as examples. A response to the bright flare is clearly distinguished for separate LOS. The normalized sum  $Sd$  of the time derivatives of the TEC variations for all LOS is presented in Figure 4c; panel (d) plots the same curve (c), upon subtracting the trend determined as a polynomial of degree 3 on the time interval 12:48-13:12 UT. Next the resulting time dependence was integrated in order to obtain the mean integral increment of TEC (Figure 4e). It might be well to point out that the time dependence of the mean integral increment of TEC has a more flattened form in the rise than the emission flux characteristics; however, the onset time of its increase coincides with that of hard

X-ray emission, and is delayed by about 1.8 minutes with respect to the UV 171 Å line.

A total of 11 events was processed. The class of X-ray flares was from M4.5 to M7.4. It was found that the mean TEC variation response in the ionosphere depends on the flare location on the Sun (central meridian distance, CMD) - Figure 5a.

## 5 Discussion

Our results is consistent with the findings reported by (Donnelly, 1969), (Donnelly, 1971), (Donnelly, 1976), (Donnelly et al., 1986a), where a study of extreme UV (EUV) flashes of solar flares observed via SFD was made. In the cited references it was shown that the relative strength of impulsive EUV emission from flares decreases with increasing CMD and average peak frequency deviation is also significantly lower for SFD's associated with  $H\alpha$  flares at large CMD. (Donnelly, 1971) is of the opinion that percentage of  $H\alpha$  flares with SFD's tends to decrease for large CMD of  $H\alpha$  flare location - Figure 5b. Similar effects at the center and limb were observed in the ratio of EUV flux to the concurrent hard X ray flux (Kane and Donnelly, 1971). Using a fourth-order polynomial to fit the results in Figure 5b with CMD in degrees (Donnelly, 1976) gives

$$A(CMD) \simeq 1 - 0.484 \cdot CMD + 0.001426 \cdot CMD^2 - 1.79 \cdot 10^{-5} CMD^3 + 7.43 \cdot 10^{-8} CMD^4 \quad (5)$$

Equation (5) implies that on the average the impulsive EUV emission is more than an order of magnitude weaker for flares near the solar limb than for flares at the central meridian. (Donnelly, 1976) have assumed that it is result from the low-lying nature of the  $10^4 K - 10^6 K$  flare source region and from absorption of EUV emission in the surrounding cool nonflaring atmosphere. Figure 5c presents the result of a modeling of the SFD occurrence probability at the time of the solar flare as a function of CMD (solid line) in arbitrary units, as well as the values amplitude of the TEC response in the ionosphere to solar flares (in the range of X-ray class M4.9-M5.7 (dots), and M6.6-M7.4 (grosses) as a function of CMD. The modeling used equation (5). It figure suggests that the results of our measurements do not contradict the conclusions drawn by Donnelly (1976) that the relative strength of impulsive EUV emission from flares decreases with increasing CMD. It should be noted that in the case of solar flares whose class is similar in X-ray emission, the dependence under study resembles  $\cos(CMD)$  rather than a polynomial of degree 4. The fitting  $\cos(CMD)$  curve for solar X-ray M4.4-M5.7 flares is plotted in Figure 5a (solid line) and 5c (dashed line). This conclusion is consistent with the findings reported by (Donnelly and Puga, 1990). In the cited reference it was found the empirical curves of the average dependence

of active region emission on its CMD (Figure 6a) for several wavelengs. Assume a quiet Sun plus one average active region that starts at the center of the backside of the Sun and rotates across the center of the solar disk with a 28-day period.

Fig. 6(b-e) presents our obtained dependencies of  $\Delta I$  as a function of the angular distance of the flaring region from the central solar meridian (CMD) for different classes of flares in the X-ray range: X2.0-X5.7 (Fig. 6b, 6 flares), M2.0-M7.4 (Fig. 6c, 26 flares), M1.1 (Fig. 6d, 14 flares), and C2.7-C10 (Fig. 6e, 7 flares). Because of lack of space, we do not give here any detailed characteristics of the flares. Our analysis was based on using sets of GPS stations and LOS similar to those described in the previous section. Fig. 6a presents the appropriate dependencies of X-ray flux emission intensities (Mosher, 1979), F10 cm (Riddle, 1969; Vauquois, 1955), and UV (Samain, 1979).

It is evident from Fig. 6 that the character of the response amplitude corresponds to the behavior of ultraviolet lines. Hence it follows that the main contribution to the ionospheric TEC response to solar flares is made by the F region and the upper part of the E region where solar ultraviolet radiation is absorbed.

Fig. 7 plots, on a logarithmic scale, the dependence of the response amplitude  $\Delta I$  to solar flares as a function of their peak power  $F$  in the X-ray range for flares located near the center of the solar disk ( $CMD < 40^\circ$ ). This dependence illustrates a wide dynamic range of the proposed method (three orders in the flare power), and is quite well approximated by the power-law function

$$\Delta I = 649.4 \cdot F^{0.7} \quad (6)$$

## 6 SUMMARY

This paper suggests a new method for investigating the ionospheric response to faint solar flares (of X-ray class C) when the variation amplitude of the TEC response to individual LOS is comparable to the level of background fluctuations. The dependence of the TEC variation response amplitude on the flare location on the Sun is investigated. In the case of solar flares whose class is similar in X-ray emission, the dependence under study resembles  $\cos(CMD)$ . The high sensitivity of our method permits us to propose the problem of detecting, in the flare X-ray and EUV ranges, emissions of non-solar origins which are the result of supernova explosions. For powerful solar flares it is not necessary to invoke a coherent summation, and the ionospheric response can be investigated for each beam. This opens the way to a detailed study of the SID dependence on a great variety of parameters (latitude, longitude, solar zenith angle, spectral characteristics of the emission flux, etc.). With current increasing solar activity, such studies become highly challenging. In addition to solving traditional problems of estimating parameters of ionization processes in the ionosphere and problems of reconstructing



emission parameters, the data obtained through the use of our method can be used to estimate the spatial inhomogeneity of emission fluxes at scales of the Earth's radius.

## 7 Acknowledgements

Authors are grateful to E.A. Kosogorov and O.S. Lesuta for preparing the input data. Thanks are also due V.G. Mikhalkovsky for his assistance in preparing the English version of the manuscript. This work was done with support under RFBR grant of leaping scientific schools of the Russian Federation No. 00-15-98509 and Russian Foundation for Basic Research (grants 99-05-64753, 00-05-72026, 00-07-72026 and 00-02-16819a), GNTF 'Astronomy'.

## References

- [1] Afraimovich, E. L., 2000a. GPS global detection of the ionospheric response to solar flares, *Radio Science*, 35, 1417–1424.
- [2] Afraimovich, I. L., Kosogorov E. A. and Leonovich L. A., 2000b. The use of the international GPS network as the global detector (GLOBDET) simultaneously observing sudden ionospheric disturbances, *Earth, Planets, and Space*, 52, 1077–1082.
- [3] Afraimovich, E.L., A.T. Altyntsev, E.A. Kosogorov, N.S. Larina, and L.A. Leonovich, 2001. Detecting of the Ionospheric effects of the solar flares as deduced from global GPS network data, *Geomagnetism and Aeronomy*, 41, 2, 208–214.
- [4] Aschwanden M. W., Fletcher L., Schrijver C. J., and Alexander. D., 1999. Coronal loop oscillation observed with the transition region and coronal explorer, *Astrophys. J.*, 520, 810 – 894.
- [5] Calais E. and J. B. Minster, 1996. GPS detection of ionospheric perturbations following a Space Shuttle ascent, *Geophys. Res. Lett.*, 23, 1897–1900.
- [6] Davies K., 1990. *Ionospheric radio*, Peter Peregrinus, London, 580 pp.
- [7] Davies K., 1980. Recent progress in satellite radio beacon studies with particular emphasis on the ATS-6 radio beacon experiment, *Space Sci. Rev.*, 25, 357.
- [8] Deshpande S. D. and Mitra A. P., 1972. Ionospheric effects of solar flares, IV, electron density profiles deduced from measurements of SCNA's and VLF phase and amplitude, *J. Atmos. Terr. Phys.* 34, 255.

- [9] Donnelly R. F., 1969. Contribution of X-ray and EUV bursts of solar flares to Sudden frequency deviations, *J. Geophys. Res.*, 74, 1873 – 1877.
- [10] Donnelly R. F., 1971. Extreme ultraviolet flashes of solar flares observed via sudden frequency deviations: experimental results, *Solar physics*. 20, 188–203
- [11] Donnelly R. F., 1976. Empirical models of solar flare X-ray and EUV emission for use in studying their E and F region effects, *J. Geophys. Res.* 81, 4745–4753.
- [12] Donnelly R. F., Hinteregger H. E., Heath D. F., 1986a. Temporal variations of solar EUV, UV, and 81.830 Å radiations, *J. Geophys. Res.*, 91, 5567 – 5578.
- [13] Donnelly R. F., Puga, L. C., and Busby, W. S., 1986b., NOAA Tech. Memo. ERL ARL-146, NOAA ERL, Boulder, Colo.
- [14] Donnelly R. F. and Puga L.C. 1990. Thirteen-day periodicity and the center-to-limb dependence of UV, EUV and X-ray emission of Solar activity, *Solar Phys.*, 130, 369 – 390.
- [15] Hofmann-Wellenhof, B., Lichtenegger, H., and Collins, J., 1992. Global Positioning System: Theory and Practice, Springer-Verlag Wien New York, pp. 327.
- [16] Gurtner, W., RINEX: The Receiver Independent Exchange Format Version 2. <http://igscb.jpl.nasa.gov:80/igscb/data/format/rinex2.txt>, 1993.
- [17] Klobuchar, J. A., 1986. Ionospheric time-delay algorithm for single-frequency GPS users, *IEEE Transactions on Aerospace and Electronics System* AES 23(3), 325–231.
- [18] Klobuchar, J. A., 1997. Real-time ionospheric science: The new reality, *Radio Science* 32, 1943–1952.
- [19] Jones T. B., 1971. VLF Phase anomalies due to a solar X-ray flare, *J. Atmos. Terr. Phys.*, 33, 963.
- [20] Kane S.R. and Donnelly R. F., 1971. Impulsive hard X-ray and ultraviolet emission during solar flares, *Astrophys. J.*, 164, 151 – 163.
- [21] Liu J. Y., Chiu C.S., and Lin C. H., 1996. The solar flare radiation responsible for sudden frequency deviation and geomagnetic fluctuation, *J. Geophys. Res.*, 101, 10855–10862.
- [22] Mosher, J. M., 1979. The height structure of solar active regions at X-Ray wavelengths as deduced from OSO-8 limb crossing observations, *Solar. Phys.*, 64, 109.

- [23] Mendillo, M., and J.V. Evans, 1974a. Incoherent scatter observations of the ionospheric response to a large solar flare, *Radio Science*, 9, 197-203.
- [24] Mendillo M., Klobuchar J. A., Fritz R. B., da Rosa A.V., Kersley L., Yeh K. C., Flaherty B. J., Rangaswamy S., Schmid P. E., Evans J. V., Schodel J. P., Matsoukas D. A., Koster J. R., Webster A. R., Chin P., 1974b. Behavior of the Ionospheric F Region During the Great Solar Flare of August 7, 1972, *J. Geophys. Res.*, 79, 665–672.
- [25] Mitra A. P., 1974. Ionospheric effects of solar flares, D.Reidel, Norwell, Mass., 249 pp.
- [26] Ohshio M., 1971. Negative sudden phase anomaly, *Nature* 229, 239.
- [27] Riddle A.C., 1969. The quiet and slowly varying components of 9.1 cm radio emission during the solar minimum, *Solar.Phys.*, 7, 434.
- [28] Samain, D., 1979. Solar continuum data on, absolute intensities, center to limb variations and laplace inversion between 1400 and 2100 Å, *Astron. Astrophys.*, 74, 225.
- [29] Sao K., Yamashita M., Tanahashi S., Jindoh H. and Ohta K., 1970. Sudden enhancements (SEA) and decreases (DSA) of atmospherics, *J. Atmos. Terr. Phys.* 32, 1567.
- [30] Stonehocker G. H., 1970. Advanced telecommunication forecasting technique in AGY, 5th., Ionospheric forecasting, AGARD Conf. Proc., 29, 27.
- [31] Thome, G.D and L.S.Wagner, 1971. Electron density enhancements in the E and E regions of the ionosphere during solar flares, *J.Geophys. Res.*, 76, 6883–6895.
- [32] Vauquois B., 1955. *Acad. Sci. Paris C. R.*, 240, 1862.

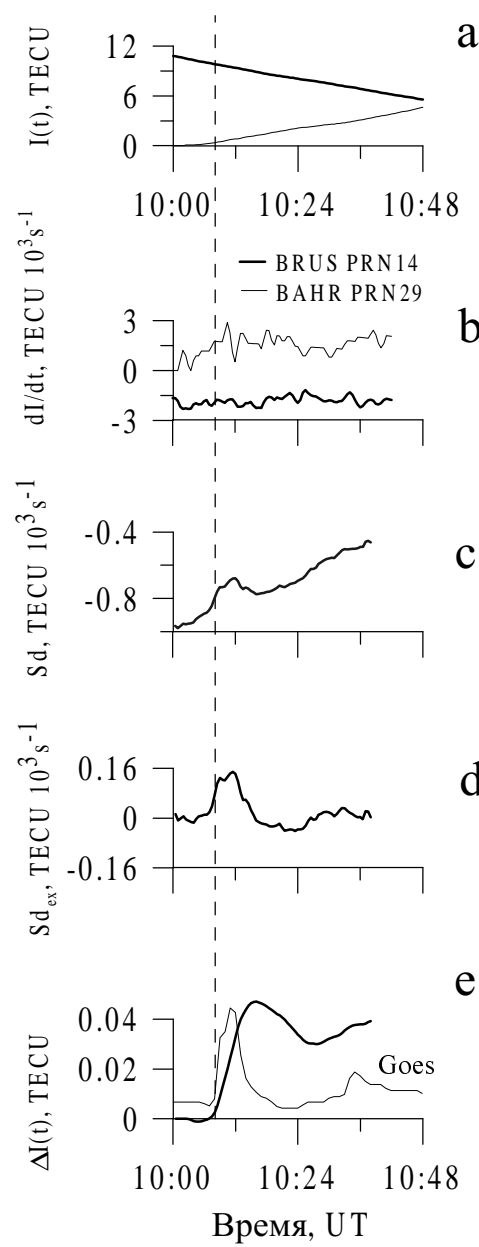


Fig.1. Faint solar flare July 29, 1999 (C2.5/SF, 10:11 UT, S16W11). The typical time dependencies of TEC variations for separate LOS (a) and their time derivatives (b) for stations BRUS (PRN14, thick line) and BAH (PRN29, thin line); a normalized result of a coherent summation  $S_d$  of the time derivatives of the TEC variations for all LOS - c; the same curve (c), upon subtracting the trend determined as a polynomial of degree 3 on the time interval 10:07-10:19 UT -d; mean integral increment of TEC (thick line) and soft X-ray emission flux (GOES-10) in the range 1-8 Å (thin line)-e.

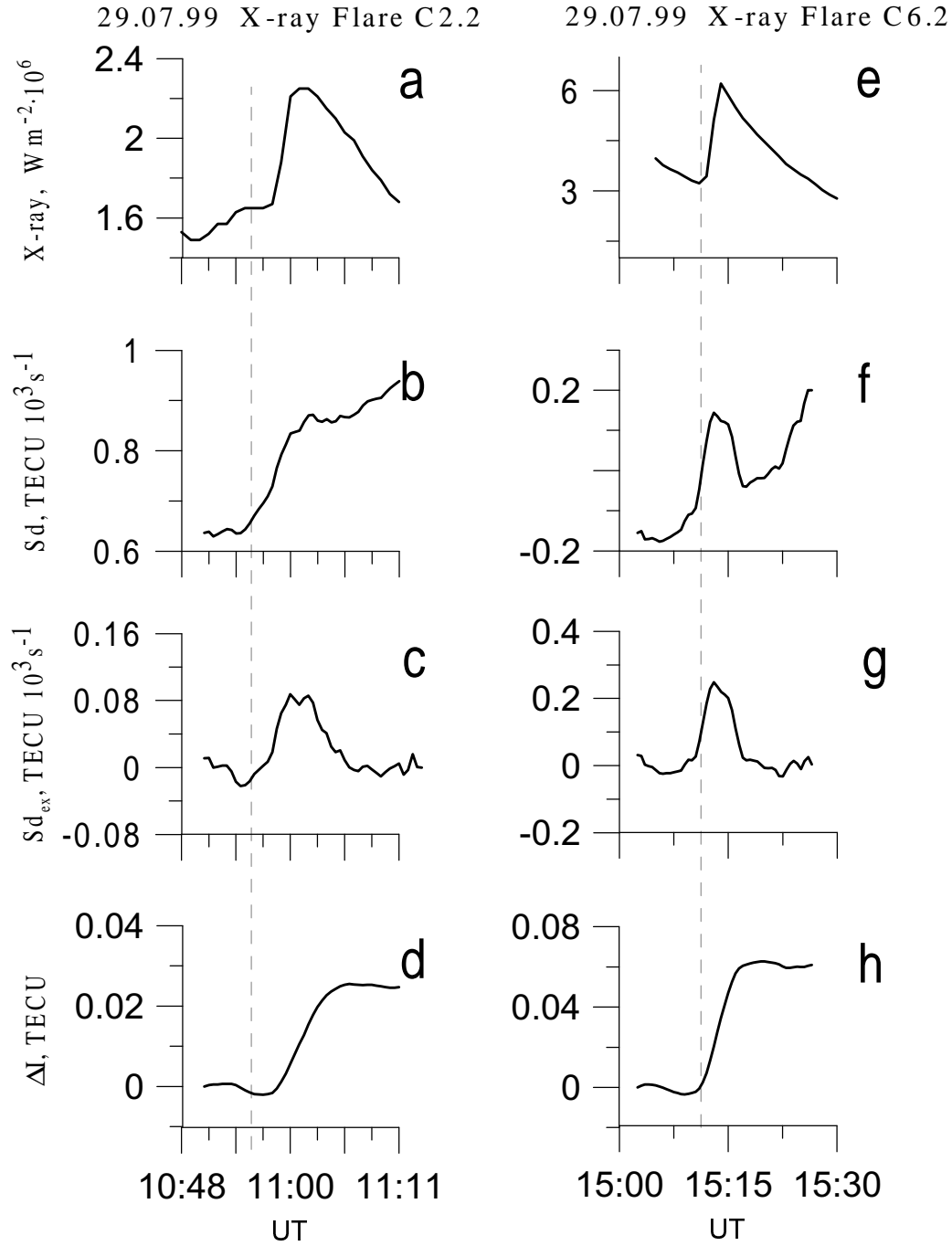


Fig. 2. Faint solar flare July 29, 1999 (C2.2, 11:00 UT), a - d; soft X-ray emission flux (GOES-10) in the range 1-8 Å - a; normalized result of a coherent summation  $S_d$  of the time derivatives of the TEC variations for all LOS - b; the same curve (b), upon subtracting the trend determined as a polynomial of degree 3 on the time interval 10:48-11:11 UT; mean integral increment of TEC - d. Analogous dependencies for faint solar flare July 29, 1999 (C6.2/SN, 15:14 UT, N25E53) on panels - e, f, g, h.

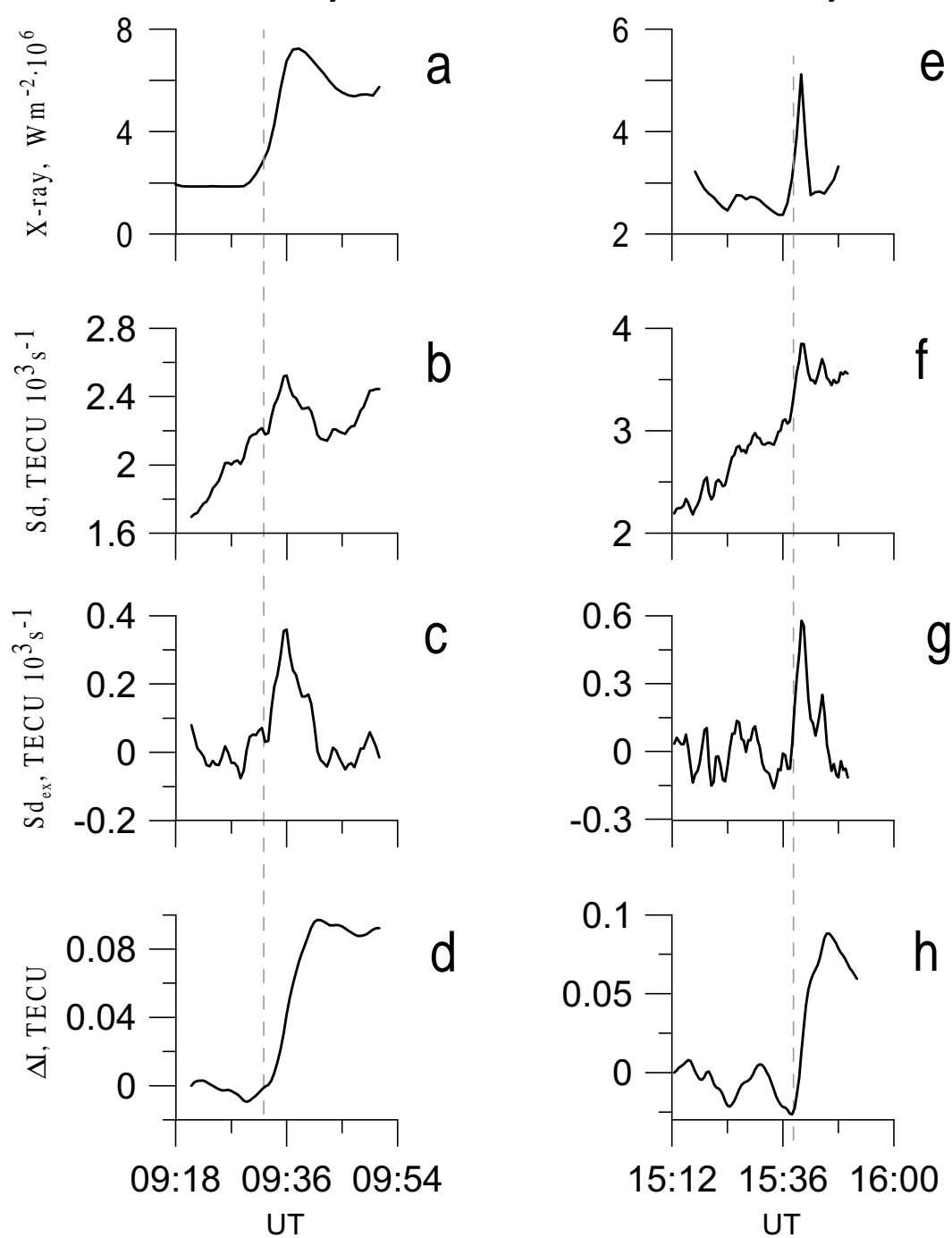


Fig.3. Faint solar flare November 17, 1999 (C7.0/1N, 09:38 UT, S15W53 ), a - d; soft X-ray emission flux (GOES-10) in the range 1-8 Å - a; normalized result of a coherent summation  $S_d$  of the time derivatives of the TEC variations for all LOS - b; the same curve (b), upon subtracting the trend determined as a polynomial of degree 3 on the time interval 09:18-09:54 UT - c; mean integral increment of TEC - d. Analogous dependencies for faint solar flare November 14, 1999 (C5.0, 15:40 UT) on panels - e, f, g, h.

14.07.98 X-ray Flare M4.6

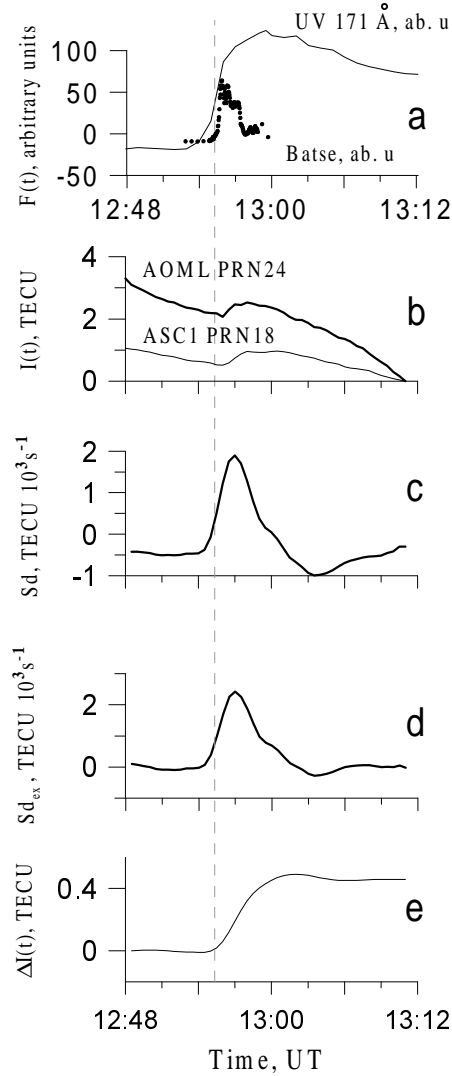


Fig. 4. Bright solar flare July 14, 1998 (12:59 UT, M4.6/1B,S23E20). Time dependencies of hard X-ray emission (CGRO/Batse, 25-50 keV, thick line) and of the UV line (SOHO/SUMMER 171 Å, thin line) in arbitrary units - a; typical time dependencies of the TEC variations for separate LOS for stations AOML (PRN24, thick line) and ACSI (PRN18, thin line) - b; the normalized sum  $S_d$  of the time derivatives of the TEC variations for all LOS - c; same curve (c), upon subtracting the trend determined as a polynomial of degree 3 on the time interval 12:48-13:12 UT - d; the mean integral increment of TEC - e.

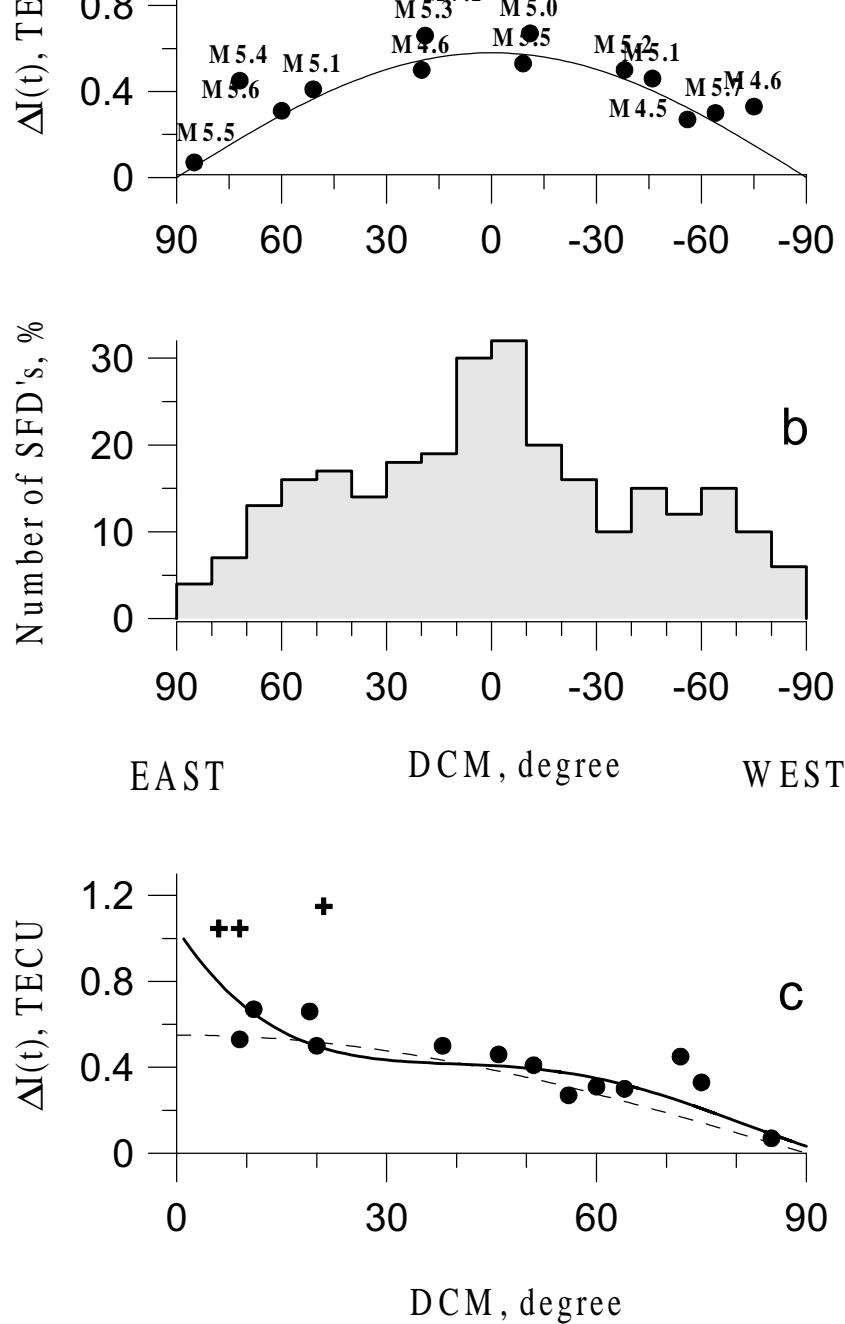
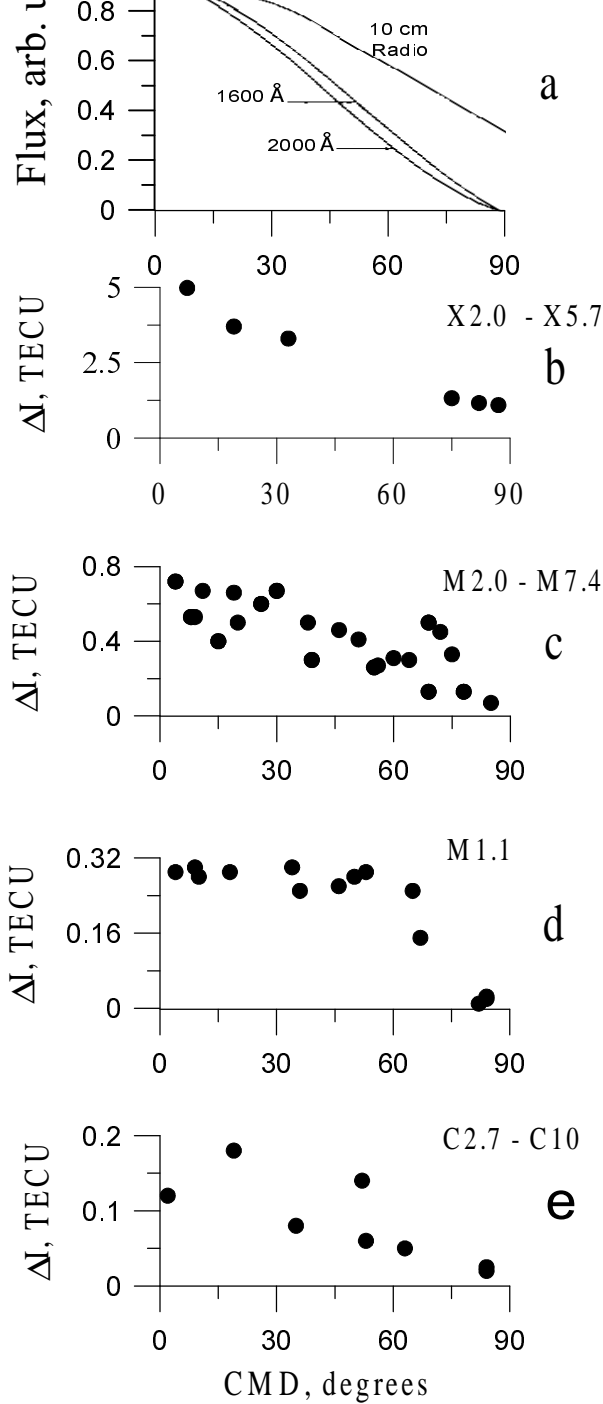


Fig. 5. CMD dependence of the increment of the mean amplitude of the TEC response to solar flares (in the range of X-ray class M4.5-M5.7 (dots), and M6.6-M7.4 (crosses);  $\cos(\text{CMD})$  fitting curve for solar flares in the X-ray range M4.5 - M5.7 (solid line) - a; percentage of Ha - flares accompanied by SFD's as a function of the central meridian distance of the Ha flare - b; modeling results on the SFD occurrence probability at the time of the solar flare as a function of the CMD (solid line), values of the mean amplitude of the TEC response in the ionosphere to solar flares (dots and crosses), and  $\cos(\text{CMD})$  fitting curve for solar flares in the X-ray range M4.5-M5.7 (dashed line) - c.





The dependencies of X-ray flux emission intensities (Mosher, 1979), F10 cm (Riddle, 1969; Vauquois, 1955), and UV (Samain, 1979) - a; The dependencies of response amplitude  $\Delta I$  as a function of the angular distance of the flaring region from the central solar meridian (CMD) for different classes of flares in the X-ray range: X2.0-X5.7 (b), M2.0-M7.4 (c), M1.1 (d), and C2.7-C10 (e).

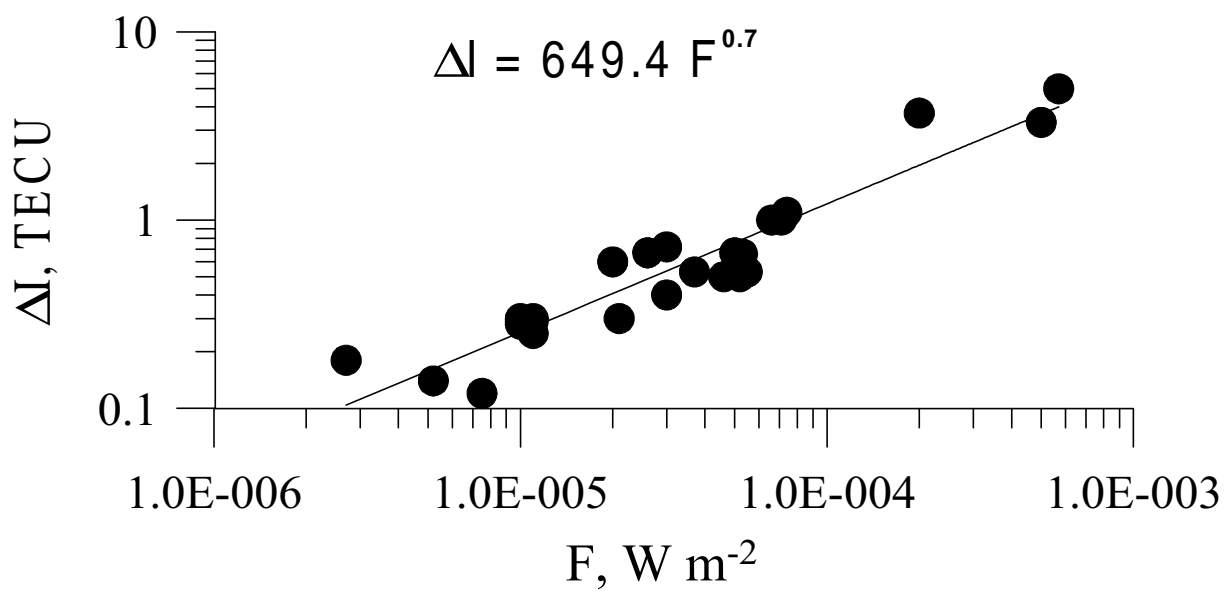


Fig.7. The dependence of the response amplitude  $\Delta I$  to solar flares as a function of their peak power  $F$  in the X-ray range.